*Article*

# Melanoma Growth Analysis in Blood Serum and Tissue Using Xenograft Model with Response to Cold Atmospheric Plasma Activated Medium

**Manish Adhikari** [1,†] **, Bhawana Adhikari** [1,†] **, Neha Kaushik** [2] **, Su-Jae Lee** [2] **, Nagendra Kumar Kaushik** [1,*] **and Eun Ha Choi** [1,*]

1   Plasma Bioscience Research Center, Applied Plasma Medicine Center, Department of Electrical and Biological Physics, Kwangwoon University, Seoul 01897, Korea; manishadhikari85@gmail.com (M.A.); bnegi87@gmail.com (B.A.)

2   Department of Life Science, Hanyang University, Seoul 04763, Korea; neha.bioplasma@gmail.com (N.K.); sj0420@hanyang.ac.kr (S.-J.L.)

*   Correspondence: kaushik.nagendra@kw.ac.kr (N.K.K.); ehchoi@kw.ac.kr (E.H.C.)

†   Both authors have equally contribution and are joint first authors in manuscript.

check for updates

**Abstract:** Background: Cold atmospheric plasma (CAP) proposed as a novel therapeutic tool for the various kinds of cancer treatment. Cold atmospheric Plasma-Activated Media (PAM) has exhibited its promising application in plasma medicine for the treatment of cancer. Methods: We investigated the role of PAM on the human melanoma cancer G-361 cells xenograft *in vivo* by estimating the biochemical and gene expression of apoptotic genes. Results: Reactive oxygen and nitrogen species (RONS) generated by PAM could significantly decrease the tumor volume (40%) and tumor weight (26%) when administered intradermally (i.d.) into the melanoma region continuously for three days. Biochemical studies in blood serum along with excised melanoma samples revealed an increase in protein carbonylation and MDA content as compared to the control, while LDH and L-DOPA in serum and melanoma tissues were decreased significantly in PAM treated group. PAM generated RONS increased apoptotic genes like *Bcl-2*, *Bax*, *Parp*, *Casp8,* and *P53* in melanoma tissue. Immunohistochemistry data confirms that PAM treatment increased apoptosis at the tissue level. Conclusions: These results suggested that RONS present in PAM inhibit the induction of xenograft melanoma cancer cells through the induction of apoptosis and upregulating of various biochemical parameters within blood serum and melanoma.

**Keywords:** cold atmospheric plasma activated medium; biochemical studies; melanoma; reactive oxygen and nitrogen species

## 1. Introduction

The extent rate of melanoma is rising consistently and faster than any other malignancy over the last few years worldwide [1]. In South Korea only, the incidence rate of cutaneous melanoma in women increased continuously every year due to poor prognosis at advanced stages of the disease [2]. Patients diagnosed with melanoma in its later stages have limited treatment possibilities, and intermediate survival ranges from 6 to 12 months in clinical trials [3]. Despite the restricted treatment options over the past few years, some molecular targeted and immune therapies are in regular practice to diagnose and treat melanoma [4–6]. Presently, the US Food and Drug Administration (FDA) has approved a combination of drugs to treat advanced-stage melanoma. Most of them contain Interleukin-2 and dacarbazine in different combinations, but a very low percentage of patients respond to them [3]. Some researchers recently discovered and claimed that the mixture of chemical compounds showed

promising potential activity against malignant melanoma, like vemurafenib (zelboraf), dabrafenib (Tafinlar), and encorafenib (Braftovi), that primarily interact with the BRAF gene and inhibit its activity [7–9]. Nowadays, standard therapies for actual melanoma treatment are using certain immunotherapies. Apart from BRAF, immunosuppression of the antitumor immune response by certain immune regulatory molecules and processes, such as T-lymphocyte-associated antigen 4 (CTLA4) and programmed cell death 1 (PD-1), is of great interest [10].

In the past few years, cold atmospheric plasma (CAP) has emerged as an effective tool for treatment against several kinds of cancers [11]. The most important aspect of anticancer therapy is the selective eradication of cancer cells without influencing healthy cells [12]. Cold plasma plays a pivotal role in maintaining this cellular homeostasis [13]. CAP acts as a plasma medicine in the biological system because of the production of partially ionized clouds of ions, electrons, and reactive neutral species, like reactive oxygen species (ROS), hydroxyl radicals (OH•), and nitrogen dioxide ($NO_2$), by its direct application [14]. Further studies revealed by some researchers concluded that cancer cells are more sensitive to its destructive effect than normal cells, which help CAP as a promising application in cancer therapy [15–17]. Another aspect of plasma medicine depends on its indirect application (off-site treatment) in which CAP is applied to some liquid medium, which leads to an increase in the reactive species within the liquid, and hence, helps in the reduction of cancer and other dreadful diseases [16]. After the CAP treatment, the plasma-treated liquid is possessed with numerous long-lived RONS, which can be retained from hours to several days, and hence, can act as a replaceable agent of CAP where direct CAP treatment is not possible [18]. Plasma-Activated Media (PAM) generates some short-lived reactive species like OH radicals, which induced apoptosis in both extracellular (culture medium) and intracellular [19]. These short-lived species lead to the development of long-lived species, like $H_2O_2$, which acts as an effective apoptosis inducer and can be applied to treat cancer cells [20,21]. In recent times, new and advanced techniques have been used in the management of melanoma reduction to understand the disease behavior and help in the development and testing of novel therapeutic strategies. As a different approach to treating melanoma, our previous publication showed promising results of the use of CAP and PAM when used with silymarin nanoemulsion in *in vitro* and *in vivo* studies [22]. For the biological aspects of understanding melanoma, animal models contributed greatly as a useful tool for testing possible treatment approaches.

Hence, for the present study, we selected Balb/c (CAnN.Cg-Foxn1nu) male nude mice (5 weeks; 22 ± 2 gm), which is the most relevant and successful animal model, in part, to our broad knowledge, for transplantation models, including the xenograft of human cancer cells [23]. The animal is kept in sterile conditions with recommended feed and sterile water inside an animal house and sacrificed in an ethical way after finishing the experiments. Various melanoma biomarkers and genes were studied using blood serum and melanoma samples extracted from the animal and kept at −80 °C for the study.

Henceforth, the main focus of this study is to assess an anti-melanoma therapeutic method by a CAP treated medium (PAM) using a µ-dielectric barrier discharge (µ-DBD) plasma device having air as the feeder gas. The results demonstrate the significant physiological changes (decreased tumor weight and volume), along with the upregulation of protein carbonylation and malondialdehyde (MDA) levels, which are the key damaging biomarkers of melanoma progression. Also, the level of Lactate Dehydrogenase (LDH) and L-3,4-dihydroxyphenylalanine (L-DOPA), which is the intermittent product of the melanin synthesis pathway, is reduced after giving the PAM treatment. The gene analysis of apoptotic related genes (*Akt*, *Bcl-2*, *Bax*, *Parp*, *Casp8,* and *P53*), along with other results, revealed the role of PAM as an anti-melanoma agent in nude mice. Hence, these outcomes exhibited the conceivable role of PAM *in vivo* to inhibit the progress of melanoma.

## 2. Materials and Methods

### 2.1. Chemicals and Animal

RPMI-1640, phosphate-buffered saline, and penicillin-streptomycin antibody cocktail solution were obtained from Welgene, Korea. Trichloroacetic acid, thiobarbituric acid, formalin, xylene, hematoxylene, eoisin, canada balsam, tris, sodium pyrophosphate, sodium orthovanadate, chloroform, and ethanol were purchased from Sigma-Aldrich, Gyeonggi-do, Korea. Protein carbonylation kit, *P53* antibody, *Parp* antibody, *Bcl-2* antibody, *Casp8* antibody, and *Akt* antibody were obtained from Abcam, Cambridge, MA, USA. Lactate dehydrogenase kit was purchased from Bioassays systems, Cambridge, MA, USA. L-DOPA analysis kit was procured from Mybiosource, Cambridge, MA, USA. RNAiso plus (Trizol) was purchased from Takara, Shiga, Japan. Isoropanol was purchased from Thermofisher, Seoul, Korea. Diethyl pyrocarbonate (DEPC) was obtained from Biosesang, Gyeonggi-do, Korea. ReverTra Ace® qPCR RT Master Mix c-DNA synthesis kit was purchased from Toyobo, Osaka, Japan. SYBR Green Master mix was procured from Bio-Rad, Seoul, Korea. All the primers for q-PCR studies were obtained from Searchbio, Seoul, Korea, and the Balb/c nude mice (CAnN.Cg-Foxn1nu) were ordered from Orientbio, Gyeonggi-do, Korea, respectively.

### 2.2. Device Characteristics and PAM Production

A CAP μ-dielectric barrier discharge (μ-DBD) surface plasma device consisting of electrodes with a silicon dioxide ($SiO_2$) dielectric layer (30 mm) and hydration-prevention layers consisting of aluminium oxide and a magnesium oxide (MgO) layer was used to make the PAM. The electrode gap was fixed at 200 mm. To generate the plasma, air was used as a feeder gas into the device at a flow rate of 1.5 lpm, and a 2 mm distance was maintained between the plasma source and the upper surface of the cell culture medium (RPMI) [24]. The air CAP treatment time was restricted to 10 min, and the freshly made PAM was used for the experiment.

### 2.3. Melanoma Xenograft Induction

Human melanoma cells (G-361, $1 \times 10^6$ cells/100 μL) were introduced intradermally by injecting into the right hind flank of CAnN.Cg-Foxn1/ nude mice (Male; 5 weeks age; Orientbio, Gyeonggi-do, Korea; *n* = 6 in each group). The mice were randomly divided into a treatment group and control group when tumor size achieved to 100 $mm^3$. After attaining the recommended tumor size, treated group mice received 200 μL of PAM every day for four days by subcutaneous injection at the tumor site. The control group received the same volume of cell culture medium (RPMI-1640) as a vehicle in the right flank. The body weights were estimated on each subsequent day after the injections of the tumors, and tumor sizes were measured with vernier calipers (calculated volume = shortest diameter$^2$ × longest diameter/2) at two-day intervals. The mice were kept in a controlled environment and supplemented with the suggested animal feed and autoclaved water, which was replaced every day after proper cleaning. This study was reviewed and approved by the Institutional Animal Care and Use Committee (IACUC) of the Center for Laboratory Animal Sciences, the Medical Research Coordinating Center. Blood was withdrawn by puncturing the retro-orbital plexus nerve of the mice exactly before sacrifice (cervical dislocation) for serum collection. The melanoma was excised and stored at −80 °C for further studies (Figure 1).
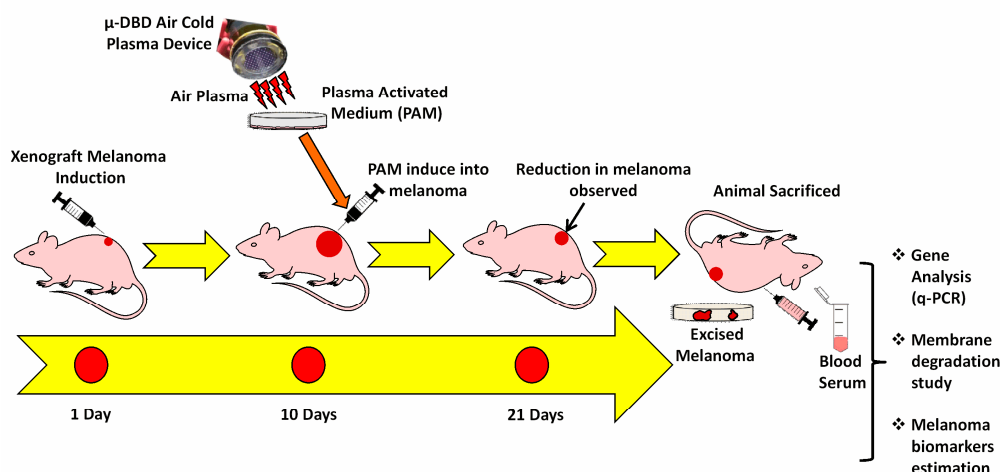
**Figure 1.** Schematic representation of human melanoma xenograft induction (G-361) and treatment strategies by cold atmospheric plasma (CAP) activated medium (Plasma-Activated Media (PAM)) in nude mice. Melanoma and blood were extracted from the mice on the 21st day for further experiments.

*2.4. Protein Carbonylation Assay*

Total protein was isolated from the excised melanoma tumor (100 mg) by homogenizing in an extraction buffer (40 mM tris, 5 mM sodium pyrophosphate, and 10 mM sodium orthovanadate) using a mortar and pestle, which was further lysed in a sonicator. Protein was pelleted by using a centrifuge at 10,000 g for 5 min at 4 °C. Protein determination was carried out using the standard Bradford protein determination assay [25]. The protein carbonylation was then quantified using a protein carbonylation kit (Abcam, Cambridge, MA, USA following the manufacturer's instruction.

*2.5. Lipid Peroxidation Estimation (MDA Content)*

Melanoma tissue membrane degradation studies were estimated by the level of MDA content and were measured spectrophotometrically by the slightly modified procedure proposed by Heath and Packer [26]. Excised melanoma was homogenized in 0.25% (*w/v*) 2-thiobarbituric acid (TBA) prepared in 10% (*w/v*) Trichloroacetic acid (TCA) in the ratio of 1:10. After that, the homogenate was incubated in a water bath at 95 °C for 30 min. This reaction mixture allowed to cool at room temperature and was centrifuged at 12,000 g for 30 min. Finally, the supernatant was collected, and its absorbance was measured at 532 nm and 600 nm. Absorbance at 600 nm was subtracted from the absorbance at 532 nm for non-specific absorbance. A 0.25% (*w/v*) 2-thiobarbituric acid (TBA) prepared in 10% (*w/v*) TCA solution was used as a blank. The concentration of MDA was calculated by using an extinction coefficient of 155 mM-1 cm-1. The content of MDA was expressed in $nM \cdot g^{-1}$ fresh weight of melanoma sample.

*2.6. LDH Assay*

LDH is a cytosolic enzyme that is an indicator of cellular toxicity and is a well-known biomarker of malignant melanoma. The LDH enzyme quantification was performed using blood serum. The serum was separated from the blood at room temperature from the blood before the starting of the experiments. The experiment was followed as per the manufacturer protocols (Bioassays systems, California, MA, USA).

*2.7. L-DOPA Estimation*

L-DOPA is the melanin precursor, and its increased concentration directly correlates with the melanoma malignancy. For L-DOPA estimation (~1 mL), blood was collected in a 1.5 mL centrifuge tube and kept for 30 min at 37 °C. After that, the blood sample was centrifuged at 1500 rpm for

10 min and serum was collected in a separate tube and stored at −80 °C until further analysis. The experimental procedure to estimate L-DOPA was followed as per the manufacturer protocols (Mybiosource, California, CA, USA).

*2.8. Real-Time q-PCR Analysis*

Total RNA was isolated from melanoma samples using RNAiso plus (Takara, Shiga, Japan). Reverse transcription (RT)-PCR was performed using ReverTra Ace® qPCR RT Master Mix c-DNA synthesis kit (Toyobo, Osaka, Japan) according to the manufacturer's instructions. Real-time PCR was performed using a CFX96™ Real-Time System (Bio-Rad, Seoul, Korea), and the results were expressed as the fold change calculated using the ΔΔCt method relative to a control sample. 18-s RNA was used as an internal normalization control. All primers were purchased from Searchbio, Gyeonggi-do, Korea. The primers used in the study are listed below in Table 1.

**Table 1.** List of primers used for the study. 18s RNA was kept as the endogenous control for the q-pcr experiment. (F = forward primer; R = Reverse Primer).

| Name | Sequence (5′–3′) |
|---|---|
| *18s RNA F* | CAGGTCTGTGATGCCCTTAGA |
| *18s RNA R* | GCTTATGACCCGCACTTACTG |
| *P53 F* | GCCCCTCCTCAGCATCTTATC |
| *P53 R* | AAAGCTGTTCCGTCCCAGTAG |
| *Bax F* | AAGAAGCTGAGCGAGTGTCTC |
| *Bax R* | GCTGGCAAAGTAGAAAAGGGC |
| *Casp8 F* | CCCAAATCAACAAGAGCCTGC |
| *Casp8 R* | TCAGACAGTATCCCCGAGGTT |
| *Akt F* | CAAAGAAGTCAAAGGGGCTGC |
| *Akt R* | TGTAGCCAATGAAGGTGCCAT |
| *Parp F* | GGTAATTGGGAGAGGTAGCCG |
| *Parp R* | TCCCCACAGACACAACACAAA |
| *Bcl-2 F* | CCACCAAGAAAGCAGGAAAC |
| *Bcl-2 R* | GCAGGATAGCAGCACAGGAT |

*2.9. Immunohistochemistry and Western Blot Analysis*

The melanoma tissue was excised from the animals of each group and fixed in formalin for the preparation of the paraffin sections. It was then deparaffinized in xylen, and then with 100%, 90%, 80%, and 70% ethanol, followed by treatment with phosphate-buffered saline (PBS). Tumor sections were stained with hematoxylin dye and counterstained with eosin dye (H&E). Afterwards, tumor sections were immunostained overnight at 4 °C with the *P53* antibody (1:300; Abcam, Cambridge, MA, USA), the *Parp* (1:300; Abcam), the *Bcl-2* (1:200; Abcam) antibody, *Casp8* (1:200; Abcam) antibody, and *Akt* (1:200; Abcam) antibody. After washing in PBS, a 1:200 dilution of biotinylated goat anti-rabbit IgG or anti-mouse IgG antibody in a blocking solution was applied to the sections. After the PBS treatment, ABC reagent was applied to the sections and incubated for 1 h. After hematoxylin counterstaining and clearing with a graded ethanol series and xylene, sections were mounted with Canada balsam. Images were photographed using an IX71 microscope (Olympus Tokyo, Japan) equipped with the DP71 digital imaging system (Olympus). For western blot analysis proteins were extracted and using SDS-PAGE, were separated and blotted into nitrocellulose membrane. Furthermore, samples were incubated with the primary antibodies overnight at 4 °C; anti-*Parp-1*, anti-*Casp8*, anti-*Akt*, anti-*P53* and anti-*β-actin*. The blots were developed using horseradish peroxidase-conjugated secondary antibodies at room temperature for 2h and anticipated using chemiluminescence procedures.

### 2.10. Statistical Analysis

Data were expressed as the mean ± SD of triplicates. All the studies were performed 3 times in triplicates ($n = 3$). The statistical significance of the difference between the values of the control and treatment groups was determined using Student's $t$-tests, and in each case, the levels of significance are indicated as * $p < 0.05$; $\delta$ $p < 0.01$; and # $p < 0.001$.

## 3. Results

### 3.1. Cold Plasma Characteristics

The µ-DBD plasma device using air as feeder gas was used for the study to make PAM at a flow rate of 1.5 lpm. It contains a conventional inbuilt inverter which operated in the dimming mode. This µ-DBD plasma is known to produce more reactive species when interacting with the liquid cell culture media [24]. In brief, the optical emission spectroscopy showed the dominant spectra of $N_2$ and weak spectra of hydroxyl radicals. The device on-time and off-time values were set constant to 33.84 ms and 86.95 ms with a duty ratio of 26%.

### 3.2. PAM Inhibited Melanoma Growth in Vivo

To check the effect of PAM on the *in vivo* model, the human melanoma cells (G-361 cells) ($1 \times 10^6$) were introduced intradermally (i.d.) into the right flank of the Balb/c nude mice (CAnN.Cg-Foxn1nu) (six animals in each group). The PAM treatment decreased the tumor volume in mice as compared to the control group (Figure 2A), as well as resulted in a reduction of the tumor weight as compared to control (Figure 2B,C). The data was acquired at the end of the experiment (21st day).
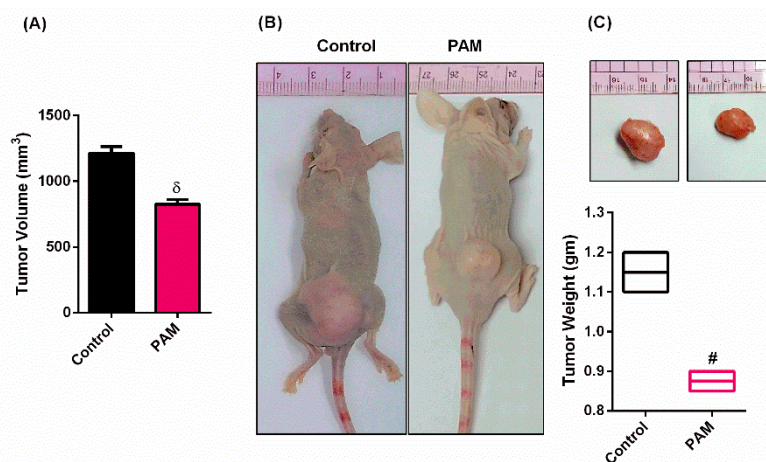


**Figure 2.** Anti-melanoma effect of PAM treatment in mice model. (**A**) Changes in the tumor volume of xenograft mice models. (**B**) Physiological observation of control and PAM treated nude mice bearing subcutaneous tumors on the right hind flank. (**C**) Photographs of solid melanoma excised from control and treatment mice on the 21st day of the study are shown above the respective bar graphs. Bar graph shows the mean tumor weight of the excised control and PAM treated melanoma. Data are mean ± SD of the mean, $n = 3$. * $p < 0.05$; $\delta$ $p < 0.01$, # $p < 0.001$.

### 3.3. PAM Induced Oxidative Damage in Melanoma (Protein and Lipid Level)

PAM contains various kinds of long-lived RONS created by the cold plasma and amalgamation of cold plasma with the medium, which leads to oxidative stress within cells. This oxidative stress leads to changes in normal redox homeostasis within the cells. To determine the redox status in the induced melanoma, mice were treated with PAM and two biomarkers of oxidative stress (protein carbonylation and lipid peroxidation) were measured spectrophotometrically. The result indicates that the level of protein carbonyl in the control sample was around 13 nmol per mg of protein (Figure 3A).

Treatment with PAM to the tumor significantly increased up to 2 times (27 nmol carbonyl per mg of protein) (Figure 3A), which indicates the induction of oxidative stress in melanoma by PAM treatment. RONS concentration enhanced by PAM, which induced oxidative damage, resulted in an increase in protein carbonylation.
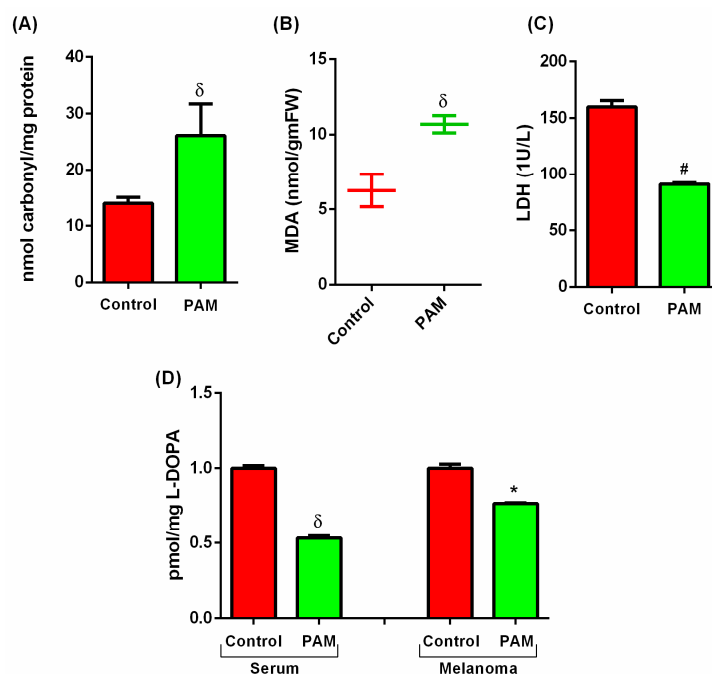


**Figure 3.** PAM induced oxidative damage and prognostic marker expressions in mice model; (**A**) protein carbonyl content estimation; (**B**) assessment of lipid peroxidation by the estimation of Malonedialdehyde (MDA) level; (**C**) lactate dehydrogenase (LDH) level, and (**D**) L-3,4-dihydroxyphenylalanine (L-DOPA) level. Blood serum and melanoma samples were collected on the 21st day of the experiment and stored at −80 °C. Data are mean ± SD of the mean, $n = 3$. * $p < 0.05$; $^{\delta}$ $p < 0.01$, # $p < 0.001$.

Lipid peroxidation is the oxidation of the lipid membrane by ROS, also enhanced by the application of PAM. MDA is a product of lipid peroxidation, which is formed by the autoxidation by free radical reaction generated by PAM. The induction in lipid peroxidation and MDA was detected by thiobarbituric acid reactive substances (TBARS) and expressed in nmol/gm of fresh weight of the melanoma tissue. In this study, it has been observed that PAM increases the MDA level. The analysis of the membrane-damaging potential of PAM revealed a significant (two times) increase in the formation of MDA as compared to the control samples (Figure 3B).

*3.4. Estimation of Melanoma Prognostic Markers Using PAM*

LDH is known as one of the prognostic markers of melanoma, which can be evaluated in blood serum [27]. In the present study, the results showed that the level of LDH in mice blood serum of the control group was high. However, the amount of LDH was drastically decreased (~50%) by the PAM treatment as compared to the control (Figure 3C). The L-DOPA was estimated in blood serum and melanoma tissue. In the blood serum of PAM treated mice, L-DOPA decreased significantly and was almost 50% lower as compared to the control mice. Though, in melanoma samples, its level also decreased marginally (7%) (Figure 3D). Several *in vitro* studies suggested that L-DOPA is toxic to dopaminergic cell cultures [28,29]. The reduced level of L-DOPA in PAM treated animals suggests that the plausible reduction in melanoma is due to the eventual reduction in melanoma pigment.

### 3.5. Gene Expression Study of Melanoma In-Vivo

The melanoma gene expression study was performed to evaluate the effect of PAM induced ROS at the molecular level. The gene expression study via q-PCR showed the increase in apoptotic gene expression in PAM treated melanoma as compared to the control mice (Figure 4C–F).
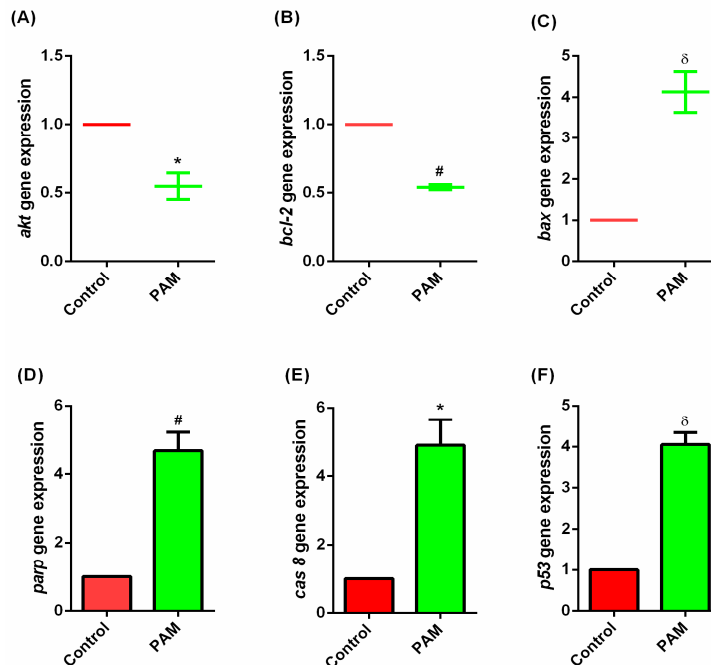


**Figure 4.** Gene expression study of melanoma cells. mRNA (*Akt, Bcl-2, Bax, Parp, Casp8, P53*) expression changes during PAM treatment on the 21st day. Bars plotted represent the mean and SD of the mean, $n = 3$, * $p < 0.05$; $^\delta$ $p < 0.01$, # $p < 0.001$.

Previous studies using CAP alone revealed the inhibition of cancer growth with treatment time [30]. The mechanism prevailing this observation is still unknown, but reactive oxygen and nitrogen species play an important role in it [31]. In this study, q-PCR was used to detect the influence of PAM treatment on melanoma-associated mRNA gene expression. As shown in Figure 4, PAM treatment significantly increases apoptotic gene expression. Specifically, the mRNA expression of *Bax* (3-fold), *Parp* (3.68-fold), *Casp8* (3.9-fold), and P53 (3-fold) increased after PAM treatment when compared to the untreated control after the 21st day of PAM administration. However, in support of the above, *Akt* and *Bcl-2* gene expression were decreased half-fold (Figure 4A,B), which strongly supports and evidently proves that PAM is able to promote apoptosis in melanoma.

### 3.6. Immunohistochemistry of Melanoma Xenograft

The histological differences in the xenograft tumor sections between the control and PAM co-treated and untreated groups were checked by immunohistochemistry (IHC) (Figure 5A). The nuclei were found to be highly condensed (apoptotic cell death) in the co-treated groups, as compared to untreated controls observed using a hematoxylin stain. We assessed the IHC score which revealed that *Parp*, *Bcl-2*, and *CASP-8* levels were significantly increased compared to those in the control group, while the expression level of *Akt* was significantly decreased in the co-treated group (Figure 5B). It was reported that p53 and *Parp* activation by CAP generated RONS leads to tumor suppression by DNA damage [32,33]. PAM treatment increased in *Parp* activation in IHC, as well as in the western blot studies, signifying defects in the double-strand DNA repair mechanism and, subsequently, referring to an increase in cellular *Casp8* (Figure 5B,C). Increase in Caspase 8 in gene levels, as well as using IHC, reveals that PAM treatment leads to xenograft melanoma cell damage, which leads to an induction of

apoptosis. The IHC provides confirmation of the decrease in apoptotic antigens within the xenograft melanoma tissues in the PAM receiving group as compared to the control group, which confirms the anti-tumor effects of PAM.
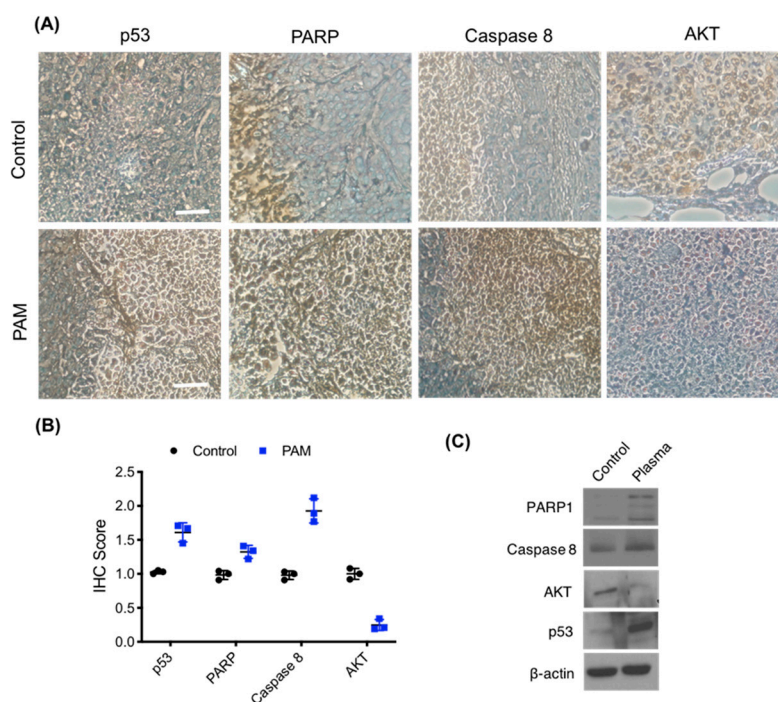


**Figure 5.** Antitumor effect of PAM in mice model. (**A**) Representative hematoxylin and eosin (H & E) staining of tissue sections of both groups (magnification, × 40). Immunohistochemical analysis of *p53*, *Parp*, *Casp-8,* and *Akt* expression levels in control and PAM treated tumors tissues. Three independent slides were checked in each case. Scale bar = 100 μm. (**B**) Graphical representation of IHC score of both groups. (**C**) Western blot analysis for *p53*, *Parp*, *Casp 8*, and *Akt*. ß-Actin is used for normalization.

## 4. Discussion

Recent studies claimed the important role of CAP in various kinds of cancer treatments. Nowadays, CAP-induced RONS, or its derived short and long-lived free radical species on interaction with liquid (in case of PAM), might be a key factor leading to anticancer effects [34]. Our *in vivo* results suggested a decrease in tumor volume and tumor weight after 21 days when giving PAM intradermally at the tumor site. This could be attributed due to the effect of the conversion of short-lived $OH^\bullet$ into long-lived hydrogen peroxide ($H_2O_2$) inside the PAM. $H_2O_2$ is the main stable species responsible for most of the activity in PAM [35]. It interacts with some other organic peroxides, which may disrupt the permeability of the melanoma cell membrane and cause cell injury, followed by an invasion of extracellular reactive species from PAM. Studies on breast cancer cell lines demonstrated the role of $H_2O_2$ and $OH^\bullet$ radical-induced apoptosis after plasma treatment [19]. These reactive species not only initiated a molecular cascade of generating cellular apoptosis but also initiated certain immunogenic treatment approaches, like the release of Damage Associated Molecular Patterns (DAMPs) or inducing Immunogenic Cell Death (ICD) and macrophage activation, which helps in the reduction of melanoma progression inside the body [36–43].

The redox reactions are very important sources of energy in the biological system, and its alteration leads to cell death [44]. PAM changed the normal machinery of the tumor by alleviating protein carbonylation, which is an irreversible post-translational modification induced by oxidative stress [45]. Another very important component, nitric oxide (NO), present in PAM (NO-PAM) accumulates inside the cells and quickly converts to $NO_2^-$ and $NO_3^-$ in PAM [46]. $NO_2^-$ to $H_2O_2$ gives a synergistic effect and reacts to produce peroxinitrite ($ONOO^-$), which is toxic and leads to protein carbonylation in

cells [47]. PAM also showed an increase in lipid peroxidation, which was estimated by the increase in MDA concentration, which directly relates to the cell in response to induced oxidative stress [48]. Excessive RONS formation (specially OH$^\bullet$) can cause macromolecule oxidation, such as membrane lipids, by abstracting a hydrogen atom from the methylene group, thus leading to the cross-linking of the fatty-acid side chain to form transient pores in the cell membrane, leading to membrane lipid peroxidation and depolarization of cell membrane potential [49].

Melanoma showed some very peculiar, effective prognostic markers, which helps melanoma cells to differentiate it from normal tissues [50]. The level of LDH and l-DOPA both decreased significantly as compared to their respective controls. LDH is responsible for the interconversion of pyruvate to lactate during glycolysis and gluconeogenesis and gives energy to the cancer cells [51]. PAM can be attributed to the reduction in LDH level because of the presence of the OH$^\bullet$ radical, which is the only important species known to inactivate the LDH effect [52], which correlates with decreased tumor burden, and hence, consequently decreases the tumor's growth and invasive potential. L-DOPA (levodopa) is a crucial intermittent chemical compound, which is a precursor of the biological pigment melanin and is produced from L-tyrosine using the enzyme tyrosine hydroxylase (tryosinase) [53]. The overexpression of L-DOPA is directly related to the excessive synthesis of melanin pigment and will lead to melanoma at later stages [54]. Molecular mechanisms associated with the CAP anti-cancer effect have been addressed in several studies. PAM is known to selectively kill glioblastoma brain tumor cells by activating *Pi3k/Akt* and *Ras/Mapk* pathways [36,55].

PAM also showed here to activate apoptotic pathways by alleviating many apoptotic related genes, which were studied using q-PCR. Intracellular reactive oxygen species present in PAM can cause DNA damage by oxidization, changing the hydrogen bonds between the complementary bases, and hence, activates poly(ADP-ribose) polymerase-1 (*Parp-1*), which further results in the decrease of intracellular ATP, leading to cell death [56]. Another biomolecule presented in PAM, which has large implications in cancer therapy, is NO. NO is well known to be a powerful agent for long-term activity against a variety of cancers [57] and could be responsible for the elevation of other apoptotic genes for melanoma suppression. Our results also prevailed in the apoptotic nature of PAM by activating the extrinsic pathway of apoptosis by increasing the *Casp 8* activity [58]. The increased level of *P53* directly relates to the *Parp* activation, which is responsible for cellular damage and hence helps in tumor suppression [59]. IHC studies also revealed an increase in the uptake of apoptotic antibodies, which signifies the potent role of PAM in melanoma reduction *in vivo*.

## 5. Conclusions

In the present study, we tried to enlighten the effect of PAM on melanoma in *in vivo* conditions via observing the change at the biochemical and molecular level in melanoma tumors and blood serum of mice. We developed a new perspective to understand the mechanism of PAM for treating melanoma. The PAM contains ROS, which induces the intracellular ROS level and activates the *P53*-signalling cascade, which consequently causes cancer cell death through activating apoptotic gene expression and degrading macromolecules. The accumulation of the RONS inside the PAM makes it a better treatment option against cancer cells as compared to CAP (Figure 6). Oxidative damage caused by PAM in protein and lipid levels were checked in melanoma tissue, and its outcome showed a decrease in their levels, respectively. The specific prognostic markers (LDH and L-DOPA) present in the blood serum and melanoma samples also revealed the decrease in the expression level of markers. The IHC of melanoma samples showed the intense expression of apoptotic markers and confirmed the significant effect of PAM on melanoma regression. Though the multifaceted mechanism networks between PAM and cell interactions (intracellular and extracellular) still need to be revealed, these findings provide significant insight into the intracellular molecular mechanism of PAM-mediated melanoma apoptosis, especially with regard to the selective killing effect. Understanding the molecular mechanism will provide strong evidence and lead to clinical applications of PAM in the future.
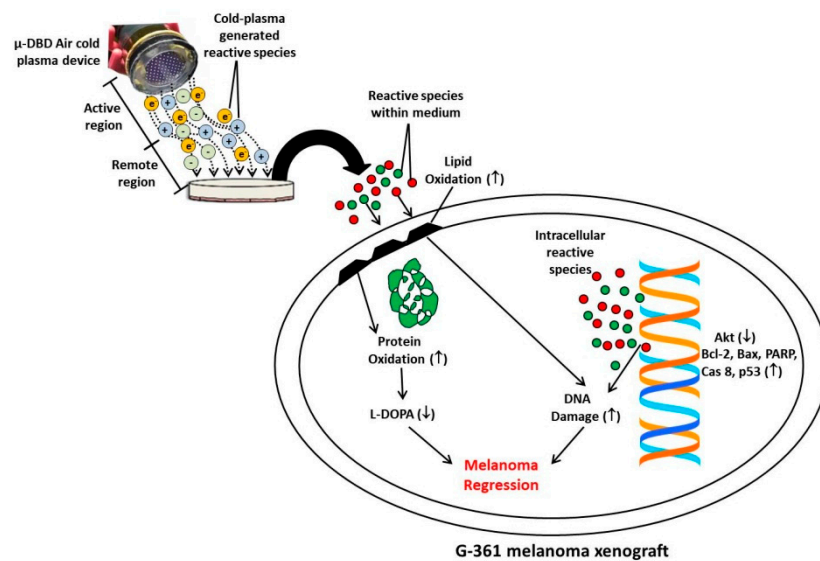
**Figure 6.** Plausible mechanism of PAM-induced damage or alteration in the G-361 melanoma xenograft in mice model.

## References

1. Giblin, A.V.; Thomas, J.M. Incidence, mortality and survival in cutaneous melanoma. *J. Plast. Reconstr. Aes.* **2007**, *60*, 32–40. [CrossRef] [PubMed]
2. Oh, C.M.; Cho, H.; Won, Y.J.; Kong, H.J.; Roh, Y.H.; Jeong, K.H.; Jung, K.W. Nationwide Trends in the Incidence of Melanoma and Non-melanoma Skin Cancers from 1999 to 2014 in South Korea. *Cancer Res. Treat.* **2018**, *50*, 729–737. [CrossRef] [PubMed]
3. Flaherty, K.T. Narrative review: Braf opens the door for therapeutic advances in melanoma. *Ann. Intern. Med.* **2010**, *153*, 587–591. [CrossRef] [PubMed]
4. Chapman, P.B.; Hauschild, A.; Robert, C.; Haanen, J.B.; Ascierto, P.; Larkin, J.; Dummer, R.; Garbe, C.; Testori, A.; Maio, M.; et al. Improved survival with vemurafenib in melanoma with BRAF V600E mutation. *N. Engl. J. Med.* **2011**, *364*, 2507–2516. [CrossRef] [PubMed]
5. Hodi, F.S.; O'Day, S.J.; McDermott, D.F.; Weber, R.W.; Sosman, J.A.; Haanen, J.B.; Gonzalez, R.; Robert, C.; Schadendorf, D.; Hassel, J.C.; et al. Improved survival with ipilimumab in patients with metastatic melanoma. *N. Engl. J. Med.* **2010**, *363*, 711–723. [CrossRef] [PubMed]
6. Hodi, F.S.; Oble, D.A.; Drappatz, J.; Velazquez, E.F.; Ramaiya, N.; Ramakrishna, N.; Day, A.L.; Kruse, A.; Mac-Rae, S.; Hoos, A.; et al. CTLA-4 blockade with ipilimumab induces significant clinical benefit in a female with melanoma metastases to the CNS. *Nat. Clin. Pract. Oncol.* **2008**, *5*, 557–561. [CrossRef]
7. Chapman, P.B.; Robert, C.; Larkin, J.; Haanen, J.B.; Ribas, A.; Hogg, D.; Hamid, O.; Ascierto, P.A.; Testori, A.; Lorigan, P.C.; et al. Vemurafenib in patients with BRAF V600 mutation-positive metastatic melanoma: Final overall survival results of the randomized BRIM-3 study. *Ann. Oncol.* **2017**, *28*, 2581–2587. [CrossRef]

8.  Brugnara, S.; Sicher, M.; Bonandini, E.M.; Donner, D.; Chierichetti, F.; Barbareschi, M.; Girardelli, C.R.; Caffo, O. Treatment with combined dabrafenib and trametinib in BRAFV600E-mutated metastatic malignant melanoma: A case of long-term complete response after treatment cessation. *Drugs Context* **2018**, *7*, 212515. [CrossRef]

9.  Koelblinger, P.; Thuerigen, O.; Dummer, R. Development of encorafenib for BRAF-mutated advanced melanoma. *Curr. Opin. Oncol.* **2018**, *30*, 125–133. [CrossRef]

10. Lo, J.A.; Fisher, D.E. The melanoma revolution: From UV carcinogenesis to a new era in therapeutics. *Science* **2014**, *346*, 945–949. [CrossRef]

11. Kufe, D.W.; Pollock, R.E.; Weichselbaum, R.R.; Bast, R.C., Jr.; Gansler, T.S.; Holland, J.F.; Frei, E., III. *Holland-Frei Cancer Medicine*, 6th ed.; BC Decker Publishing House: Toronto, ON, Canada, 2003; ISBN 1-55009-213-8.

12. Liu, J.; Wang, Z. Increased Oxidative Stress as a Selective Anticancer Therapy. *Oxid. Med. Cell. Longev.* **2015**, *2015*, 294303. [CrossRef] [PubMed]

13. Matsumoto, R.; Shimizu, K.; Nagashima, T.; Tanaka, H.; Mizuno, M.; Kikkawa, F.; Hori, M.; Honda, H. Plasma-activated medium selectively eliminates undifferentiated human induced pluripotent stem cells. *Regen. Ther.* **2016**, *5*, 55–63. [CrossRef] [PubMed]

14. Yang, H.; Lu, R.; Xian, Y.; Gan, L.; Lu, X.; Yang, X. Effects of atmospheric pressure cold plasma on human hepatocarcinoma cell and its 5-fluorouracil resistant cell line. *Phys. Plasmas* **2015**, *22*, 122006. [CrossRef]

15. Ermolaeva, S.A.; Sysolyatina, E.V.; Kolkova, N.I.; Bortsov, P.; Tuhvatulin, A.I.; Vasiliev, M.M.; Mukhachev, A.Y.; Petrov, O.F.; Tetsuji, S.; Naroditsky, B.S.; et al. Non-thermal argon plasma is bactericidal for the intracellular bacterial pathogen Chlamydia trachomatis. *J. Med. Microbiol.* **2012**, *61*, 793–799. [CrossRef]

16. Volotskova, O.; Hawley, T.S.; Stepp, M.A.; Keidar, M. Targeting the cancer cell cycle by cold atmospheric plasma. *Sci. Rep.* **2012**, *2*, 636. [CrossRef]

17. Attri, P.; Park, J.; Ali, A.; Choi, E.H. How does plasma activated media treatment differ from direct cold plasma treatment? *Anticancer Ag. Med. Chem.* **2018**, *18*, 805–814. [CrossRef]

18. Zhitong, C. Cold atmospheric plasma with self-organized patterns for cancer therapy. *Front. Nanosci. Nanotech.* **2019**, *5*, 1–4.

19. Kaushik, N.K.; Ghimire, B.; Li, Y.; Adhikari, M.; Veerana, M.; Kaushik, N.; Jha, N.; Adhikari, B.; Lee, S.J.; Masur, K.; et al. Biological and medical application of plasma-activated media, water and solutions. *Biol. Chem.* **2018**, *400*, 39–62. [CrossRef]

20. Ninomiya, K.; Ishijima, T.; Imamura, M.; Yamahara, T.; Enomoto, H.; Takahashi, K.; Tanaka, Y.; Uesugi, Y.; Shimuzu, N. Evaluation of extra- and intracellular OH radical generation, cancer cell injury, and apoptosis induced by a non-thermal atmospheric pressure plasma jet. *J. Phys. D Appl. Phys.* **2013**, *46*, 425401. [CrossRef]

21. Xiang, J.; Wan, C.; Guo, R.; Guo, D. Is Hydrogen Peroxide a Suitable Apoptosis Inducer for All Cell Types? *BioMed. Res. Int.* **2016**, *2016*, 1–7. [CrossRef]

22. Troyano, A.; Sancho, P.; Fernandez, C.; Blas, E.; Bernardi, P.; Aller, P. The selection between apoptosis and necrosis is differentially regulated in hydrogen peroxide-treated and glutathione-depleted human promonocytic cells. *Cell Death Differ.* **2003**, *10*, 889–898. [CrossRef]

23. Adhikari, M.; Kaushik, N.; Ghimire, B.; Adhikari, B.; Baboota, S.; Al-Khedhairy, A.A.; Wahab, R.; Lee, S.J.; Kaushik, N.K.; Choi, E.H. Cold atmospheric plasma and silymarin nanoemulsion synergistically inhibits human melanoma tumorigenesis via targeting HGF/c-MET downstream pathway. *Cell Commun. Signal.* **2019**, *17*, 1–14. [CrossRef] [PubMed]

24. Kuzu, O.F.; Nguyen, F.D.; Noory, M.A.; Sharma, A. Current State of Animal (Mouse) Modeling in Melanoma Research. *Cancer Growth Metast.* **2015**, *8*, 81–94. [CrossRef]

25. Kaushik, N.K.; Attri, P.; Kaushik, N.; Choi, E.H. Preliminary Study of the Effect of DBD Plasma and Osmolytes on T98G Brain Cancer and HEK Non-Malignant Cells. *Molecules* **2013**, *18*, 4917–4928. [CrossRef] [PubMed]

26. Bradford, M.M. A rapid and sensitive method for the quantitation of microgram quantities of protein utilizing the principle of protein dye binding. *Anal. Biochem.* **1976**, *72*, 248–254. [CrossRef]

27. Heath, R.L.; Packer, L. Photoperoxidation in isolated chloroplasts. I. Kinetics and Stiochiometry of fatty acid peroxidation. *Arch. Biochem. Biophys.* **1968**, *125*, 189–198. [CrossRef]

28. Balch, C.M.; Soong, S.J.; Atkins, M.B.; Buzaid, A.C.; Cascinelli, N.; Coit, D.G.; Fleming, I.D.; Gershenwald, J.E.; Houghton, A., Jr.; Kirkwood, J.M.; et al. An evidence-based staging system for cutaneous melanoma. *CA Cancer J. Clin.* **2004**, *54*, 131–149. [CrossRef] [PubMed]

29. Mena, M.A.; Pardo, B.; Casarejos, M.J.; Fahn, S.; Garcia de, Y.J. Neurotoxicity of levodopa on catecholamine-rich neurons. *Mov. Disord.* **1992**, *7*, 23–31. [CrossRef]

30. Mytilineou, C.; Han, S.K.; Cohen, G. Toxic and protective effects of L-dopa on mesencephalic cell cultures. *J. Neurochem.* **1993**, *61*, 1470–1478. [CrossRef]

31. Wang, M.; Holmes, B.; Cheng, X.; Zhu, W.; Keidar, M.; Zhang, L.G. Cold Atmospheric Plasma for Selectively Ablating Metastatic Breast Cancer Cells. *PLoS ONE* **2013**, *8*, e73741. [CrossRef] [PubMed]

32. Kalghatgi, S.; Kelly, C.M.; Cerchar, E.; Torabi, B.; Alekseev, O.; Fridman, A.; Friedman, G.; Azizkhan-Clifford, J. Effects of non-thermal plasma on mammalian cells. *PLoS ONE* **2011**, *6*, e16270. [CrossRef] [PubMed]

33. Laroussi, M. Plasma Medicine: A Brief Introduction. *Plasma* **2018**, *1*, 47–60. [CrossRef]

34. Hara, H.; Taniguchi, M.; Kobayashi, M.; Kamiya, T.; Adachi, T. Plasma-activated medium-induced intracellular zinc liberation causes death of SH-SY5Y cells. *Arch. Biochem. Biophys.* **2015**, *15*, 51–60. [CrossRef]

35. Lu, X.; Naidis, G.V.; Laroussi, M.; Reuter, S.; Graves, D.B.; Ostrikov, K. Reactive species in non-equilibrium atmospheric-pressure plasmas: Generation, transport, and biological effects. *Phys. Rep.* **2016**, *630*, 1–84. [CrossRef]

36. Boehm, D.; Curtin, J.; Cullen, P.J.; Bourke, P. Hydrogen peroxide and beyond-the potential of high-voltage plasma activated liquids against cancerous cells. *Anticancer Ag. Med. Chem.* **2017**, *18*, 815–823. [CrossRef] [PubMed]

37. Kaushik, N.K.; Kaushik, N.; Yoo, K.C.; Uddin, N.; Kim, J.S.; Lee, S.J.; Choi, E.H. Low doses of PEG-coated gold nanoparticles sensitize solid tumors to cold plasma by blocking the PI3K/AKT-driven signalling axis to suppress cellular transformation by inhibiting growth and EMT. *Biomaterials* **2016**, *87*, 118–130. [CrossRef] [PubMed]

38. Kaushik, N.K.; Kaushik, N.; Min, B.; Choi, K.H.; Hong, Y.J.; Miller, V.; Fridman, A.; Choi, E.H. Cytotoxic macrophage-release tumour necrosis factor-alpha (TNF-α) as a killing mechanism for cancer cell death after cold plasma activation. *J. Phys. D. Appl. Phys.* **2016**, *49*, 084001. [CrossRef]

39. Kaushik, N.K.; Kaushik, N.; Adhikari, M.; Ghimire, B.; Linh, N.N.; Mishra, Y.K.; Lee, S.J.; Choi, E.H. Preventing the solid cancer progression via release of anticancer-cytokines in co-culture with cold plasma-stimulated macrophages. *Cancers* **2019**, *11*, 842. [CrossRef]

40. Lin, A.; Truong, B.; Patel, S.; Kaushik, N.; Choi, E.H.; Fridman, G.; Fridman, A.; Miller, V. Nanosecond-Pulsed DBD plasma-generated reactive oxygen species triggers immunogenic cell death in A549 lung carcinoma cells through intracellular oxidative stress. *Int. J. Mol. Sci.* **2017**, *18*, 966. [CrossRef]

41. Lin, A.G.; Xiang, B.; Merlino, D.J.; Baybutt, T.R.; Sahu, J.; Fridman, A.; Snook, A.E.; Miller, V. Non-thermal plasma induces immunogenic cell death in vivo in murine CT26 colorectal tumors. *Oncoimmunology* **2018**, *7*, e1484978. [CrossRef]

42. Freund, E.; Liedtke, K.R.; van der Linde, J.; Metelmann, H.R.; Heidecke, C.D.; Partecke, L.I.; Bekeschus, S. Physical plasma-treated saline promotes an immunogenic phenotype in CT26 colon cancer cells in vitro and in vivo. *Sci. Rep.* **2019**, *9*, 1–18. [CrossRef] [PubMed]

43. Bekeschus, S.; Seebauer, C.; Wende, C.; Schmidt, A. Physical plasma and leucocytes–immune or reactive? *Biol. Chem.* **2018**, *400*, 63–75. [CrossRef] [PubMed]

44. Trachootham, D.; Lu, W.; Ogasawara, M.A.; Nilsa, R.D.; Huang, P. Redox regulation of cell survival. *Antioxid. Redox Signal.* **2008**, *10*, 1343–1374. [CrossRef] [PubMed]

45. Aryal, B.; Rao, V.A. Specific protein carbonylation in human breast cancer tissue compared to adjacent healthy epithelial tissue. *PLoS ONE* **2018**, *13*, e0194164. [CrossRef] [PubMed]

46. TAdachi, T.; Tanaka, H.; Nonomura, S.; Hara, H.; Kondo, S.; Hori, M. Plasma-activated medium induces A549 cell injury via a spiral apoptotic cascade involving the mitochondrial nuclear network. *Free Radic. Biol. Med.* **2015**, *79*, 28–44. [CrossRef] [PubMed]

47. Dalvi, S.M.; Patil, V.W.; Ramraje, N.N.; Phadtare, J.M.; Gujarathi, S.U. Nitric Oxide, Carbonyl Protein, Lipid Peroxidation and Correlation Between Antioxidant Vitamins in Different Categories of Pulmonary and Extra Pulmonary Tuberculosis. *Malays. J. Med. Sci.* **2013**, *20*, 21–30. [PubMed]

48. Barrera, G. Oxidative Stress and Lipid Peroxidation Products in Cancer Progression and Therapy. *ISRN Oncol.* **2012**, *2012*, 137289. [CrossRef] [PubMed]

49. Ferrer, E.; Juan-García, A.; Font, G.; Ruiz, M.J. Reactive oxygen species induced by beauvericin, patulin and zearalenone in CHO-K1 cells. *Toxicol. In Vitro* **2009**, *23*, 1504–1509. [CrossRef]

50. Palmer, S.R.; Erickson, L.A.; Ichetovkin, I.; Knauer, D.J.; Markovic, S.N. Circulating Serologic and Molecular Biomarkers in Malignant Melanoma. *Mayo Clin. Proc.* **2011**, *86*, 981–990. [CrossRef] [PubMed]

51. Goldman, R.D.; Kaplan, N.O.; Hall, T.C. Lactic dehydrogenase in human neoplastic tissues. *Cancer Res.* **1964**, *24*, 389–399.

52. Buchanan, J.D.; Armstrong, D.A. Free radical inactivation of lactate dehydrogenase. *Int. J. Radiat. Biol. Relat. Stud. Phys. Chem. Med.* **1976**, *30*, 115–127. [CrossRef] [PubMed]

53. Siple, J.F.; Schneider, D.C.; Wanlass, W.A.; Rosenblatt, B.K. Levodopa therapy and the risk of malignant melanoma. *Ann. Phamacother.* **2000**, *34*, 382–385. [CrossRef] [PubMed]

54. Slominski, A.; Zmijewski, M.; Pawelek, J. L-tyrosine and L-DOPA as hormone-like regulators of melanocytes functions. *Pigment Cell Melanoma Res.* **2012**, *25*, 14–27. [CrossRef] [PubMed]

55. Tanaka, H.; Mizuno, M.; Ishikawa, K.; Nakamura, K.; Utsumi, F.; Kajiyama, H.; Kano, H.; Maruyama, S.; Kikkawa, F.; Hori, M. Cell survival and proliferation signaling pathways are downregulated by plasma-activated medium in glioblastoma brain tumor cells. *Plasma Med.* **2012**, *2*, 207–220. [CrossRef]

56. Kumar, N.; Park, J.H.; Jeon, S.N.; Park, B.S.; Choi, E.H.; Attri, P. The action of microsecond-pulsed plasma-activating media on the inactivation of human lung cancer cells. *J. Phys. D Appl. Phys.* **2016**, *49*, 115401. [CrossRef]

57. Hirst, D.; Robson, T. Targeting nitric oxide for cancer therapy. *J. Pharm. Pharmacol.* **2007**, *59*, 3–13. [CrossRef] [PubMed]

58. Kominami, K.; Nakabayashi, J.; Nagai, T.; Tsujimura, Y.; Chiba, K.; Kimura, H.; Miyawaki, A.; Sawasaki, T.; Yokota, H.; Manabe, N. The molecular mechanism of apoptosis upon caspase-8 activation: Quantitative experimental validation of a mathematical model. *Biochim. Biophys. Acta* **2012**, *1823*, 1825–1840. [CrossRef] [PubMed]

59. Wiman, K.G. p53 talks to PARP: The increasing complexity of p53-induced cell death. *Cell Death Differ.* **2013**, *20*, 1438–1439. [CrossRef] [PubMed]